

Performance of Layered Steered Space–Time Codes in Wireless Systems

Ahmad S. Salim · Salam A. Zummo ·
Samir N. Al-Ghadhban

Published online: 9 May 2013
© Springer Science+Business Media New York 2013

Abstract Layered Steered Space–Time Codes (LSSTC) is a recently proposed multiple-input multiple-output (MIMO) system that combines the benefits of vertical Bell Labs space–time (VBLAST) scheme, space–time block codes (STBC) and beamforming. In this paper, we derive the error performance and capacity of a single-user LSSTC system. The analysis is general enough to any layer ordering and modulation schemes used. In addition, the derived analysis is general for any LSSTC structure in which layers may have different number of antenna arrays and may be assigned power according to any power allocation. Furthermore, we analytically investigate the tradeoff between the main parameters of the LSSTC system, i.e., diversity, multiplexing and beamforming. Our results give recursive expressions for the probability of error for LSSTC which showed nearly perfect match to the simulation results. Results have also revealed the possibility of designing an adaptive system in which it

The material in this paper was presented in part at the Personal, Indoor and Mobile Radio Communications (PIMRC) conference, Istanbul, Turkey, September 2010. In that work we have presented some of the results we had on the performance of LSSTC without giving much detail on their derivations, on the other hand, this paper gives the complete derivations of the error performance results and includes extensive comparisons between the analytical and the simulation results for the error performance, capacity and the VBLAST–LSSTC adaptive system. Another part of this paper was presented in part at the International Conference on Wireless Information Networks and Systems (WINSYS), Athens, Greece, July 2010. That work included some of the results on the capacity of an LSSTC system and how it outperforms VBLAST.

A. S. Salim (✉)
School of Electrical, Computer and Energy Engineering (ECEE),
Arizona State University, Tempe, AZ 85287–5706, USA
e-mail: ahmd.salim@gmail.com

S. A. Zummo · S. N. Al-Ghadhban
Electrical Engineering Department, King Fahd University of Petroleum and Minerals (KFUPM),
P.O. Box 7626, Dhahran 31261, Saudi Arabia

S. A. Zummo
e-mail: zummo@kfupm.edu.sa

S. N. Al-Ghadhban
e-mail: samir@kfupm.edu.sa

was shown that combining beamforming, STBC, and VBLAST has better performance than VBLAST at high SNR range.

Keywords Layered Steered Space–Time Codes · LSSTC · STBC · VBLAST · Beamforming · Capacity · Probability of error · Tradeoff

1 Introduction

Various techniques have been proposed to counter the problem of propagation conditions, and to achieve data rates that are very close to the Shannon limit. One of these techniques is using MIMO systems which uses antenna arrays at both the transmitter and the receiver. Wolniansky et al. [1] has proposed in the well-known MIMO scheme, known as VBLAST. In VBLAST architecture, parallel data streams are sent via the transmit antennas at the same carrier frequency. Given that the number of receive antennas is greater than or equal to the number of transmit antennas, the receiver employs a low complexity method based on successive interference cancellation (SIC) to detect the transmitted data streams. In this manner, VBLAST can achieve high spectral efficiencies without any need for increasing the system's bandwidth or transmitted power.

Alamouti [2] has presented in a new scheme called STBC with two transmit and one receive antennas that provides the same diversity order as maximal-ratio receiver combining (MRRC) with one transmit and two receive antennas. This scheme can be generalized to two transmit antennas and M receive antennas to provide a diversity order of $2M$. Similar work was considered in [3] where space time trellis codes (STTC) were used as the component codes. With the tempting advantages of VBLAST and STBC, many researchers has attempted to combine these two schemes to result in a multilayered architecture called multilayered space–time block codes (MLSTBC) [4] with each layer being composed of antennas that corresponds to a specific STBC. This combined scheme arises as a solution to jointly achieve spatial multiplexing and diversity gains simultaneously. With MLSTBC scheme, it is possible to increase the data rate while keeping a satisfactory link quality in terms of symbol error rate (SER) [5].

In [6] beamforming was combined with MLSTBC to produce a hybrid system called the layered steered space time codes (LSSTC). The addition of beamforming to MLSTBC further improves the performance of the system by focusing the energy towards one direction, where the antenna gain is increased in the direction of the desired user, while reducing the gain towards the interfering users.

In [7], analytical performance evaluation of VBLAST systems was conducted employing zero-forcing successive interference cancellation (ZF–SIC) without ordering and using binary phase shift keying (BPSK) over Rayleigh-fading channel. Further, a general recursive procedure to calculate the bit error rate (BER) of each sub-stream with arbitrary number of transmit and receive antennas was proposed. Similar work but in a different approach has been conducted in [8]. Up to the authors knowledge, no analysis has been derived for LSSTC systems before. It would be interesting and novel to extend this analysis to the case of LSSTC.

The LSSTC system as shown in this paper can be used as a multi-configuration MIMO downlink system, in which the BS switches between VBLAST and LSSTC schemes as well as different modulation schemes based on the channel state information (CSI) fed back from the mobile station. The used mode (whether VBLAST or LSSTC and the modulation scheme) is chosen such that the bandwidth efficiency of the transmission is the highest while achieving the target error rate.

The LSSTC system along with the proposed adaptive scheme can be added to the existing and evolving wireless communication systems that employ MIMO such as the long-term evolution (LTE) or WiMAX, seamlessly and with quite low cost. The proposed adaptive scheme can be used to optimize the performance by selecting between the VBLAST mode and the LSSTC mode with changing the modulation scheme. As seen from the numerical results, this system can result in a huge drop in the symbol error rate at a much higher bandwidth efficiency compared to either VBLAST or STBC acting alone, for instance, this system can achieve a SER as small as 10^{-8} at an SNR of 16 dB as shown in Fig. 4. This means that the system will be highly efficient and reliable.

The main contribution of this paper is the analysis of the error performance of LSSTC, in which recursive expressions for the probability of error for VBLAST from [7] are generalized to LSSTC. The analytical results are obtained for BPSK and QAM modulation schemes. Our analysis is general such that it includes asymmetric layered systems in which layers may have different number of antenna arrays and different amount of power. On the other hand, previous work such as that of [7] has assumed the system to be symmetrical in terms of power and that all the layers have a single antenna. In addition, we derive the fundamental tradeoff curves between multiplexing, diversity, and beamforming gains provided by LSSTC systems. Furthermore, we evaluate LSSTC by comparing its capacity and error rate to the VBLAST system. For that, we derive a formula for the instantaneous capacity of single-user LSSTC. Finally, an adaptive scheme that is based on LSSTC and VBLAST systems is proposed. This scheme selects the configuration and the modulation scheme in order to improve the performance.

The remainder of this paper is organized as follows. Section 2 gives a detailed description of our system model considering its components; VBLAST, beamforming, and STBC. Section 3 presents the performance analysis of LSSTC, in which we derive a formula for the probability of bit error. In Sect. 4, we derive a formula for the instantaneous capacity of single-user LSSTC. In Sect. 5, the tradeoff between several advantages of LSSTC is analyzed. Section 6 presents the simulation results conducted to evaluate the LSSTC system. Finally, conclusions are drawn in Sect. 7. Table 1 describes the general notation and summarizes the most frequent symbols and operators in this paper.

2 System Model

Figure 1 shows the block diagram of a single-user LSSTC system proposed in [6]. The system has N_T total transmitting antennas and N_R receiving antennas and is denoted by an $N_T \times N_R$ LSSTC. The antenna architecture employed in Fig. 1 has M transmit adaptive antenna arrays (AAs) spaced sufficiently far apart (greater than $d = \lambda/2$) in order to experience independent fading and hence achieve transmit diversity. Each of the AAs consists of L elements that are spaced at a distance less than $d = \lambda/2$ to ensure achieving beamforming. A block of B input information bits is sent to the vector encoder of LSSTC and serial-to-parallel converted to produce K streams (layers) of length B_1, B_2, \dots, B_K , where $B_1 + B_2 + \dots + B_K = B$. Each group of B_k bits, $k \in [1, K]$, is then encoded by a component space-time code STC_k associated with m_k transmit AAs, where $m_1 + m_2 + \dots + m_K = M$. The output of the k th STC encoder is a $m_k \times l$ codeword, \mathbf{c}_i , that is sent over l time intervals. The space-time coded symbols from all layers can be written as $\mathbf{C} = [\mathbf{c}_1, \mathbf{c}_2, \dots, \mathbf{c}_K]^T$, where \mathbf{C} is an $M \times l$ matrix.

The coded symbols from \mathbf{C} are then processed by the corresponding beamformers, and then transmitted simultaneously over the wireless channels. The transmit antennas of all the

Table 1 Notation, symbols, and operators

<i>Notation</i>	
Vectors	Bold-face, Lower-case letters
Matrices	Bold-face, Capital letters
<i>Symbols</i>	
H	Channel matrix
$\tilde{\mathbf{H}}$	The reconstructed channel matrix
e_k	Estimation error
N_T	Number of transmit antennas
N_R	Number of receive antennas
M	Number of antenna arrays
K	Number of layers (groups)
m_k	Number of antenna arrays associated with the k th STBC encoder in the k th layer
L	Number of antenna elements per antenna array
P_T	Total transmission power
P_i	The transmit power of the i th sub-stream
Y	Received baseband data matrix
W	$M \times M$ diagonal weight matrix
\mathbf{c}_k	The component STBC used at layer k
A_{k-1}^i	The event of having i errors in the symbols $\hat{S}_1 \sim \hat{S}_{k-1}$
P_{e_k}	The probability of error on the k th layer
r	Spatial multiplexing gain
d	The diversity gain
λ	The wavelength
<i>Operators</i>	
$E[\cdot]$	Expectation operator
$Cov[\cdot]$	Covariance operator
$ \cdot $	Matrix determinant
$\ \cdot\ $	Matrix Frobenius norm
$(\cdot)^H$	Hermitian
$(\cdot)^T$	Transpose
$(\cdot)^*$	Conjugate

groups are synchronized and allocated equal power. Moreover, the total transmission power is fixed, where the transmitted symbols have an average power of $P_T = 1$, where the average is taken across all codewords over both spatial and temporal components. For the LSSTC system to operate properly, the number of receive antennas N_R should be at least equal to the number of layers K .

We formulate the system model as follows. The channel model is a MIMO quasi-static Rayleigh flat-fading channel with N_T transmit antennas and N_R receive antennas. The quasi-static assumption indicates that the channel gain coefficients remain constant for the duration of the STBC block and change independently for each STBC block. The flat-fading assumption allows each transmitted symbol to be represented by a single-tap in the discrete-time model with no inter-symbol interference (ISI). We assume independent Rayleigh coefficients,

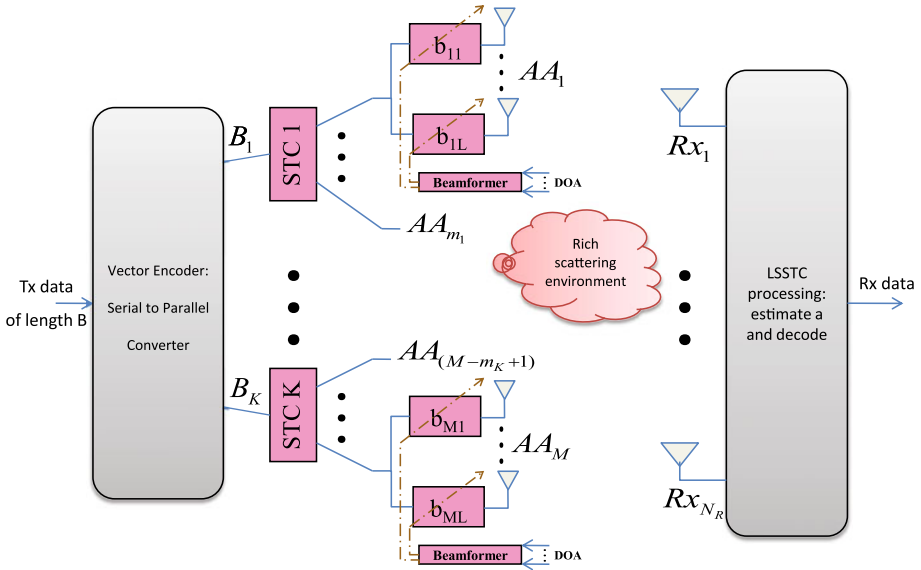


Fig. 1 Block diagram of a single user LSSTC system

i.e., fading coefficients are independent and identically distributed (i.i.d.) circular-complex normal random variables with zero-mean and 0.5 variance per dimension, abbreviated as $\mathcal{CN}(0, 1)$. The correlation caused by the small distance separation is approximately removed using the beamforming processing as we will show in this section. At the receiver, white Gaussian noise is added. The system model also assumes that the receiver has perfect channel state information (CSI), whereas the transmitter has the DOA data sent from the receiver.

Denote the L -dimensional channel impulse response (CIR) vector spanning the m th AA, $m \in [1, \dots, M]$ and the n th receiver antenna, $n \in [1, \dots, N_R]$ as $\mathbf{h}_{n,m}(t)$. Over flat fading channels $\mathbf{h}_{n,m}$ can be expressed as [9]

$$\mathbf{h}_{n,m}(t) = [\mathbf{d}_{n,m}]^T \cdot \alpha_{n,m}(t), \tag{1}$$

where $\alpha_{n,m}$ is the Rayleigh faded channel coefficient coupling the m th AA to the n th receiver antenna, and $\mathbf{d}_{n,m}$ is the adaptive antenna array response corresponding to the m th AA and the n th receiver antenna, defined as [9]

$$\mathbf{d}_{n,m} = \left[1, e^{-j2\pi d(m) \sin(\Psi_{n,m})/\lambda}, \dots, e^{-j2\pi(L-1)d(m) \sin(\Psi_{n,m})/\lambda} \right]^T, \tag{2}$$

where $d(m)$ is the distance between the elements of the m th AA, $\Psi_{n,m}$ is the nm th link's direction of arrival (DOA), and superscript ' T ' denotes the matrix transposition.

The signal model can be described in matrix notation, where the received baseband data matrix can be written as

$$\mathbf{Y} = \mathbf{HWC} + \mathbf{N}, \tag{3}$$

where \mathbf{Y} is the received signal over l time intervals and has a dimension of $N_R \times l$, \mathbf{H} is an $N_R \times M$ matrix whose entries are $\mathbf{h}_{n,m}$ defined in (1), and \mathbf{N} is an $N_R \times l$ matrix that characterizes the additive white Gaussian noise (AWGN). The n th row of \mathbf{N} denoted as \mathbf{z}_n , where $n \in [1, \dots, N_R]$, is a row vector of l columns, the i th entry of \mathbf{z}_n is a spatially

uncorrelated circular-complex normal random variable, and can be written as $z_n^i = z_{I,n}^i + jz_{Q,n}^i$, where $z_{I,n}^i$ and $z_{Q,n}^i$ are two independent zero-mean Gaussian random variables having a variance of $N_0/2$, we will represent z_n^i as $\mathcal{CN}(0, N_0)$. Furthermore, \mathbf{W} is an $M \times M$ diagonal weight matrix, whose diagonal entry $\mathbf{w}_{m,m}$ is the L -dimensional beamforming weight vector for the m th beamformer AA and the n th receive antenna, and can be written as $\mathbf{w}_{m,m} = [b_{m1}, \dots, b_{mL}]$, where b_{mi} , $i \in [1, \dots, L]$, is the i th weighting gain of the m th AA. Throughout this paper, the phrase "sub-stream" is used to refer to the data stream of each AA, whereas, the term "layer" represents the data stream to be encoded by STBC. The transmitted symbols can be written in vector form as $\mathbf{x} = [x_1, \dots, x_M]^T$, where x_i is the i th symbol (sub-stream) sent by the i th AA.

The beamforming vector $\mathbf{w}_{m,m}$ is given by [9] as $\mathbf{w}_{m,m} = \mathbf{d}_{n,m}^*$, where the superscript $*$ represents the conjugate of the matrix. In the following we will attempt to obtain some simplifications for the channel matrix; these simplifications will pave the way toward Sect. 3 and they will be vital for the logical flow of the paper. We define a modified channel matrix as

$$\hat{\mathbf{H}} = \mathbf{H}\mathbf{W} = \begin{bmatrix} \mathbf{h}_{1,1}\mathbf{w}_{1,1} & \cdots & \mathbf{h}_{1,M}\mathbf{w}_{M,M} \\ \mathbf{h}_{2,1}\mathbf{w}_{1,1} & \cdots & \mathbf{h}_{2,M}\mathbf{w}_{M,M} \\ \vdots & \ddots & \vdots \\ \mathbf{h}_{N_R,1}\mathbf{w}_{1,1} & \cdots & \mathbf{h}_{N_R,M}\mathbf{w}_{M,M} \end{bmatrix}, \tag{4}$$

where $\hat{\mathbf{H}}$ is the reconstructed channel matrix comprising the MIMO fading channel and the DOA information. Note that we assumed that the nulling vector for all the paths corresponding to one AA ($\mathbf{w}_{m,m}$) is the same. This follows from the assumption that the separation between the receive antennas is much less than the distance between the AA and the receiver, then roughly speaking, they will have the same direction of arrival, which will result in having the same nulling vector. According to Eq. (4), \mathbf{Y} can be rewritten as

$$\mathbf{Y} = \hat{\mathbf{H}}\mathbf{C} + \mathbf{N}. \tag{5}$$

The channel coefficient of the n th row and the m th column, $\hat{\mathbf{H}}(n, m)$, can be expressed as

$$\begin{aligned} \hat{\mathbf{H}}(n, m) &= \mathbf{h}_{n,m}\mathbf{w}_{m,m} \\ &= \alpha_{n,m} \cdot [\mathbf{d}_{n,m}]^T [\mathbf{d}_{n,m}]^* \\ &= L \cdot \alpha_{n,m}. \end{aligned} \tag{6}$$

Therefore the received signal can be expressed as in [6]

$$\mathbf{Y} = L\tilde{\mathbf{H}}\mathbf{C} + \mathbf{N}, \tag{7}$$

where $\tilde{\mathbf{H}}$ is an $(N_R \times M)$ matrix whose entries are $\alpha_{n,m}$. Looking at (7), the effect of beamforming can be clearly seen as a direct gain in the signal-to-noise ratio (SNR). Expressing $\tilde{\mathbf{H}}\mathbf{C}$ in terms of the layers components we get

$$\mathbf{Y} = L \sum_{k=1}^K \tilde{\mathbf{h}}_k \mathbf{c}_k + \mathbf{N}, \tag{8}$$

where \mathbf{c}_k represents the component STBC used at layer k , where $k \in [1, \dots, K]$. Further, $\tilde{\mathbf{H}}$ can be Partitioned into groups corresponding to each layer as in [4]:

$$\tilde{\mathbf{H}} = [\tilde{\mathbf{h}}_1, \dots, \tilde{\mathbf{h}}_K], \tag{9}$$

where $\tilde{\mathbf{h}}_k$ is the channel matrix of the k th layer.

On the receiver side, serial group interference cancelation (SGIC) is used to detect the signal. The detection process can be classified into two types [10]. The first type is the non-ordered detection, in which choosing the layer to be detected does not depend on the power of the layer, and the detection order is predetermined before the signal is received. The second type is the post-ordered detection, where the detection order is not known until the channel realization is perfectly estimated at the receiver. The authors of [4, 10] have proposed a procedure for the detection of layered STBC. In our work, we have generalized the procedure to any LSSTC structure. Interested readers may refer to [11] for more details on the steps of SGIC for LSSTC systems.

3 Performance Analysis of LSSTC

In this section we derive a nearly exact error probability analysis for the LSSTC with SGIC receiver. In the analysis we will consider the effect of errors propagating from the previous erroneous layers. We will analyze the system assuming that the power is unequally splitted among the layers at the transmitter. Our analysis gives recursive expressions for the error probability of each symbol which is evaluated using a recursive procedure [7]. Our analysis is generalized to cover asymmetric layers with different number of antenna arrays and different amount of power.

For the purpose of finding the probability of LSSTC error we will extend the virtual MIMO representation in [12] to LSSTC, where the received vectors from the l time slots are rearranged into one vector and the LSSTC system will be equivalent to an M -branch VBLAST system, where M is the number of AAs. For convenience the received signal obtained from (7) is re-written as

$$\underbrace{\mathbf{y}_v}_{(N_R \cdot l) \times 1} = L \underbrace{\mathbf{H}_v}_{(N_R \cdot l) \times M} \underbrace{\mathbf{x}}_{M \times 1} + \underbrace{\mathbf{n}_v}_{(N_R \cdot l) \times 1}, \tag{10}$$

where \mathbf{y}_v , \mathbf{H}_v and \mathbf{n}_v represent the virtual representation of \mathbf{Y} , $\tilde{\mathbf{H}}$, and \mathbf{N} respectively. Further, \mathbf{H}_v can be partitioned into groups corresponding to each sub-stream as $\mathbf{H}_v = [\mathbf{h}_1, \dots, \mathbf{h}_M]$. Using the received signal, the detector will perform SGIC. At the end of each stage and after subtracting the contribution of the first k detected substreams $\{x_1, \dots, x_k\}$, the updated received signal becomes

$$\begin{aligned} \mathbf{y}_v^k &= \mathbf{y}_v - L \sum_{j=1}^k \mathbf{h}_j \hat{x}_j \\ &= \underbrace{L \sum_{j=k+1}^M \mathbf{h}_j x_j}_{\text{faded target signal with interference}} + \underbrace{\left(\mathbf{n}_v + L \sum_{j=1}^k \mathbf{h}_j \cdot (x_j - \hat{x}_j) \right)}_{\text{equivalent noise}}. \end{aligned} \tag{11}$$

In (11), the vector \mathbf{y}_v^k is composed of three parts: the yet-to-be-detected symbols, the noise vector and the potential error propagation signal. We refer to the last two terms of (11) as the equivalent noise.

Assuming a total transmit power of P_T , the i th AA will have P_i as a transmit power which is a fraction of P_T . Since each AA results in a scalar $\alpha_{i,j}$ after multiplying by the weight

matrix \mathbf{W} , each AA will be treated as a single antenna for the purpose of calculating transmit power and received SNR. According to [13], if a system has M independent sub-channels, the exact probability of bit error on the k th symbol when using BPSK modulation can be expressed as

$$P_{e_k} = \left[\frac{1}{2}(1 - \mu) \right]^{D_k} \sum_{t=0}^{D_k-1} \binom{D_k - 1 + t}{t} \left[\frac{1}{2}(1 + \mu) \right]^t, \tag{12}$$

where $\mu = \sqrt{\frac{\rho}{1 + \rho}}$, ρ is the sub-stream SNR, $\rho = \frac{(LP_i)}{N_0}$, and D_k is the diversity order of the layer $\Gamma(k)$ from which the k th symbol is transmitted, and of course, all sub-streams associated with the same layer have the same diversity order, for instance, if we used Alamouti's STBC, the first and second sub-streams will have the same diversity order. Going in the same line of derivation of [1], the diversity order of LSSTC can be obtained. In [1], the authors derived an expression for the diversity order of VBLAST that results only from implementing serial detection, however, this can be extended to the case of LSSTC by noting that the diversity of each layer is now enhanced by the diversity gain of STBC, therefore we write the diversity order of the k th sub-stream as $D_k = m_{\Gamma(k)}(N_R - K + \Gamma(k))$. It can be noted that STBC increases the diversity order of each layer by the multiplicative factor $m_{\Gamma(k)}$.

It is clear to see that the generalization of this procedure to M-PSK, or M-QAM can be done simply by replacing (12) with the formulas corresponding to these modulation schemes. Note that all the sub-streams of a layer employing STBC have the same probability of error and will be assigned the same amount of power. For instance, if $m_1 = 2$, then $\text{Prob}\{x_1 \neq \hat{x}_1\} = \text{Prob}\{x_2 \neq \hat{x}_2\}$. For convenience, we refer to P_{e_k} in (12) as $P_e(D_k, \rho)$.

The sub-stream error will depend on the number of errors that occurred in the sub-stream itself and on the errors propagating from the previous layers, and will not depend on the errors occurring in the other sub-streams of the same layer. Therefore, we will calculate the layer probability of error, which will be equal to the probability of sub-stream error of the sub-streams sent from that layer. Therefore throughout this paper we will express the layer performance in terms of that of one of its substreams. For the i th layer the latter will be denoted as s_i .

For square $M_q - QAM$, the probability of symbol error in the k th symbol under Rayleigh fading can be written as follows [14]

$$P_e(D_k, \rho) = 4 \left(1 - \frac{1}{\sqrt{M_q}} \right) I_1 - 4 \left(1 - \frac{1}{\sqrt{M_q}} \right)^2 I_2, \tag{13}$$

where the terms I_1 and I_2 are defined as

$$I_1 = \left[\frac{1}{2}(1 - \mu) \right]^{D_k} \cdot \sum_{t=0}^{D_k-1} \binom{D_k - 1 + t}{t} \left[\frac{1}{2}(1 + \mu) \right]^t, \tag{14}$$

$$I_2 = \frac{1}{4} - \mu \cdot \left(\frac{1}{2} - \frac{1}{\pi} \cdot \tan^{-1}(\mu) \right) \cdot \sum_{t=0}^{D_k-1} \binom{2t}{t} \cdot (4\tau)^{-t} + \frac{\mu}{\pi} \sin(\tan^{-1}(\mu)) \sum_{t=1}^{D_k-1} \sum_{i=1}^t \tau^{-t} \cdot T_{it} \cdot (\cos(\tan^{-1}(\mu)))^{2(t-i)+1}, \tag{15}$$

where

$$\mu \triangleq \sqrt{\frac{\rho}{\frac{2}{3}(M_q - 1) + \rho}}, \tag{16}$$

$$\tau \triangleq \left(\frac{3\rho}{2(M_q - 1)} + 1 \right), \tag{17}$$

$$T_{it} \triangleq \frac{\binom{2t}{t}}{\binom{2(t-i)}{t-i} 4^i \cdot (2(t-i) + 1)}. \tag{18}$$

It is clear that in the absence of error propagation, the layer probability of error of the k th layer for $k = 1, \dots, K$, can be expressed as $P_{e_k} = P_e(D_k, \rho)$. But when considering the presence of error propagation, the probability of error can be expressed as in [7]

$$\begin{aligned} P_{e_k} &= \text{Prob}\{s_k \neq \hat{s}_k\} \\ &= \sum_{i=0}^{k-1} \text{Prob}\{s_k \neq \hat{s}_k \mid A_{k-1}^i\} \text{Prob}\{A_{k-1}^i\}, \end{aligned} \tag{19}$$

where A_{k-1}^i defines the event of having i errors in the first $(k - 1)$ detected layers. Now in order to find P_{e_k} , we need to find $\text{Prob}\{s_k \neq \hat{s}_k \mid A_{k-1}^i\}$ and $\text{Prob}\{A_{k-1}^i\}$ first, which are derived as follows

Define the equivalent noise as a new random variable $\mathbf{n}^{i,k}$ given by

$$\begin{aligned} \mathbf{n}^{i,k} &= \mathbf{n}_v \mid A_{k-1}^i \\ &= \mathbf{n}_v + L \sum_{j=1}^i \mathbf{h}_{g_k(j)} \cdot (s_{g_k(j)} - \hat{s}_{g_k(j)}) \end{aligned} \tag{20}$$

where $g_k(\cdot)$ is a map function defined to accommodate for any injection of i detection errors in the first $k - 1$ layers. Assuming BPSK modulation, $s_{g_k(j)}$ will take one of the values in the set $\{-\sqrt{P_i}, +\sqrt{P_i}\}$, and therefore, $(s_{g_k(j)} - \hat{s}_{g_k(j)})$ given that $s_{g_k(j)} \neq \hat{s}_{g_k(j)}$, will take a value from the set $\{-2\sqrt{P_i}, +2\sqrt{P_i}\}$. Note that the equivalent noise given in (20) is not Gaussian [7] since the event A_{k-1}^i will bring restrictions on \mathbf{n}_v and $\mathbf{h}_{g_k(j)}$. However, in the analysis of [7] it was assumed that $\mathbf{n}^{i,k}$ is white Gaussian, This assumption is shown to be a good approximate in [7]. It should be noted that the obtained results are approximate analysis. For example, Fig. 5a, b shows that using this assumption, the analysis curve is very close to the simulation curve, which validates the use of the Gaussian approximation analysis to the cross-layer interference. In order to completely express $\mathbf{n}^{i,k}$ assuming it is a white Gaussian random variable (RV), we need to find its mean and variance. First, let's calculate the mean of the RV $\mathbf{n}^{i,k}$:

$$\mathbb{E}[\mathbf{n}_v \mid A_{k-1}^i] = \mathbb{E}[\mathbf{n}_v] + L \sum_{j=1}^i \mathbb{E}[\mathbf{h}_{g_k(j)}] \cdot \mathbb{E}[s_{g_k(j)} - \hat{s}_{g_k(j)}]. \tag{21}$$

Since $s_{g_k(j)}$ and $\hat{s}_{g_k(j)}$ are taken from the same constellation then they have same expected value, which is zero. Therefore $\mathbb{E}[\mathbf{n}_v \mid A_{k-1}^i] = \mathbb{E}[\mathbf{n}_v] = 0$. We obtained the covariance matrix of $\mathbf{n}^{i,k}$ in [11] as $\text{Cov}[\mathbf{n}_m^{i,k}, \mathbf{n}_n^{i,k}] = [N_0 + 4i P_i L^2] I_{N_R \times N_R}$. Substituting for

Cov $\left[\mathbf{n}_m^{i,k}, \mathbf{n}_n^{i,k} \right]$, $\text{Prob}\{s_k \neq \hat{s}_k \mid A_{k-1}^i\}$ in (19) can be expressed as

$$\text{Prob}\{s_k \neq \hat{s}_k \mid A_{k-1}^i\} = P_e \left(m_k(N_R - K + k), \frac{P_i L^2}{N_0 + 4i P_i L^2} \right). \tag{22}$$

Following the analysis in [7], the expressions for $\text{Prob}\{A_{k-1}^i\}$ can be derived to be as follows.

$$\text{Prob}\{A_{k-1}^i\} = \begin{cases} \left[1 - P_e \left(m_{k-1}(N_R - K + k), \frac{P_i L^2}{N_0} \right) \right] \cdot \text{Prob}\{A_{k-2}^0\}, & i = 0 \\ \text{Prob}\{s_{k-1} \neq \hat{s}_{k-1} \mid A_{k-2}^{i-1}\} \cdot \text{Prob}\{A_{k-2}^{i-1}\} \\ + \left[1 - \text{Prob}\{s_{k-1} \neq \hat{s}_{k-1} \mid A_{k-2}^i\} \right] \cdot \text{Prob}\{A_{k-2}^i\}, & 0 < i < k - 1 \\ P_e \left(m_{k-1}(N_R - K + k), \frac{P_i L^2}{N_0 + 4P_i(k-2)L^2} \right) \cdot \text{Prob}\{A_{k-2}^{k-2}\}, & i = k - 1 \end{cases} \tag{23}$$

After finding $\text{Prob}\{s_k \neq \hat{s}_k \mid A_{k-1}^i\}$ and $\text{Prob}\{A_{k-1}^i\}$, the probability of error on the k th layer denoted as P_{e_k} can be evaluated directly using (19). From that we can find the probability of error of the individual sub-streams by $\text{Prob}\{x_m \neq \hat{x}_m\} = P_{e_{\Gamma(m)}}$, where $\Gamma(m)$ is the layer from which the m th sub-stream (x_m) is sent. The average probability of error over all M sub-streams can be written as

$$P_{av} = \frac{1}{M} \cdot \sum_{k=1}^M \text{Prob}\{x_k \neq \hat{x}_k\}. \tag{24}$$

4 Capacity of LSSTC

In [6], the authors derived and studied the average capacity of the system assuming different layer rates, Eqs. (2) and (4) in [6]. In this section, we derive the instantaneous outage capacity of the proposed system, which depends on the instantaneous channel condition. This is important to our analysis in order to evaluate the outage capacity at a given outage probability and compare it to other MIMO schemes such as VBLAST. Our assumption is that all layers have the same rate. Therefore, the outage capacity is determined by the weakest layer.

To derive a formula for the capacity of LSSTC per user we start from the capacity formulas of STBC and VBLAST. First, the instantaneous capacity was found in [15] for an orthogonal STBC. In MLSTBC which is a combination of VBLAST and STBC, an outage occurs if an outage happens in any layer because all the STBC encoders (layers) are transmitting at the same rate. The layer that is the most probable to fall in an outage is the weakest layer [16], i.e. the one that has the least value of $\|\mathbf{H}_i\|^2$, $i = 1, 2, \dots, K$, where $\|\mathbf{H}_i\|^2$ is the squared Frobenius norm of the i th matrix of \mathbf{H} . Therefore, the instantaneous capacity of a K -layered STBC system with a layer SNR of ρ can be written as

$$C = K \cdot R_s \cdot \min_{k=1,2,\dots,K} \left\{ \log_2 \left(1 + \rho \cdot \|\mathbf{H}_i\|^2 \right) \right\}. \tag{25}$$

The right hand side of (25) is originally an upper bound for the instantaneous capacity, but (25) becomes exact because of the assumption mentioned in 2 of having the antenna arrays sufficiently far from each other (larger than $\lambda/2$), which will result in having independent fading channels and this has been validated in [15]. Extending the last results, the instantaneous capacity of LSSTC can be expressed as

$$C_{LSSTC} = K \cdot R_s \cdot \min_{k=1,2,\dots,K} \left\{ \log_2 \left(1 + \frac{L \cdot P_{L,k}}{m_k \cdot N_0} \cdot \|\mathbf{H}_{PP,k}\|^2 \right) \right\} \tag{26}$$

where $P_{L,k}$ is the power assigned to the k th layer and $\mathbf{H}_{PP,k}$ is the Post-Processing (PP) matrix corresponding to the k th layer after nulling out the interference from the yet-to-be-detected layers. It is clear that the LSSTC capacity is dominated by the worst group which has the minimum value of $\|\mathbf{H}_{PP,k}\|^2$, $k = 1, 2, \dots, K$.

In Sect. 6, we compare the LSSTC outage capacity with that of VBLAST as shown in Fig. 6. This comparison is important to justify the LSSTC system and explore the tradeoffs between LSSTC and VBLAST.

5 Diversity, Multiplexing, and Beamforming Tradeoff

In [17] the authors have found the tradeoff curve for a MIMO system that has the capability of providing both diversity and multiplexing advantage. In this section, we generalize this analysis to the beamforming advantage of LSSTC by providing a comparison among different LSSTC system configurations. A system is said to have a diversity gain of d if the error probability decays as $(SNR)^{-d}$ [17], and a spatial multiplexing gain of r if the rate of the scheme is $(r \log SNR)$.

In an LSSTC system with N_T transmit and N_R receive antennas, assuming the path gains between individual antenna pairs are i.i.d. Rayleigh faded, the maximum diversity gain ignoring the antennas assigned for beamforming is $\left(\frac{N_T N_R}{L}\right)$, which is the total number of fading realizations over which system performance is averaged. The tradeoff curve shows the diversity advantage achievable by the LSSTC system for each multiplexing gain r , and beamforming gain which we define as the number of beamforming elements (L). Clearly, L cannot exceed the total number of transmit antennas N_T . On the other hand, r cannot exceed the total number of degrees of freedom provided by the channel $\min\left(\frac{N_T N_R}{L}, N_R\right)$; and $d(r, L)$ cannot exceed the maximum diversity gain of the channel $\left(\frac{N_T N_R}{L}\right)$. The tradeoff curve links between these three extreme limits. The tradeoff curve is found in a similar manner to [17], and is given by the piecewise-linear function connecting the points $(r, d(r, L))$, $r = 0, 1, \dots, \min\left\{\frac{N_T N_R}{L}, N_R\right\}$. For each possible value of L , the diversity gain $d(r, L)$ is given by

$$d(r, L) = \left(\frac{N_T}{L} - r\right)(N_R - r) \tag{27}$$

Figure 2a shows the diversity-multiplexing tradeoff curve of a 16×8 LSSTC system. As we can see from the figure, two points of interest can be identified

$$d_{max} = d(r_{min}, L_{min}) = d(0, 1) = \frac{N_T N_R}{L} \tag{28}$$

$$r_{max} = \min\left\{\frac{N_T N_R}{L}, N_R\right\} \tag{29}$$

It can be noted that increasing the diversity advantage at a specific beamforming gain comes at a price of decreasing the spatial multiplexing gain, and vice versa. Figure 2b shows the diversity-beamforming tradeoff of a 16×8 LSSTC system. In Fig. 2a it should be noted that the points to the left of each curve represent an achievable diversity gain for that specific configuration, whereas the points to the right are not achievable. This means that we may

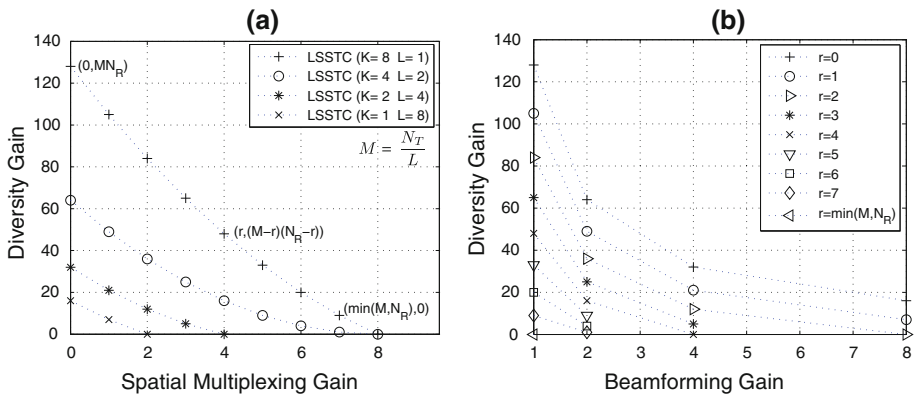


Fig. 2 **a** Diversity-multiplexing tradeoff of a 16×8 LSSTC with $m_k = 2$, and **b** diversity-beamforming tradeoff of a 16×8 LSSTC with $m_k = 2$

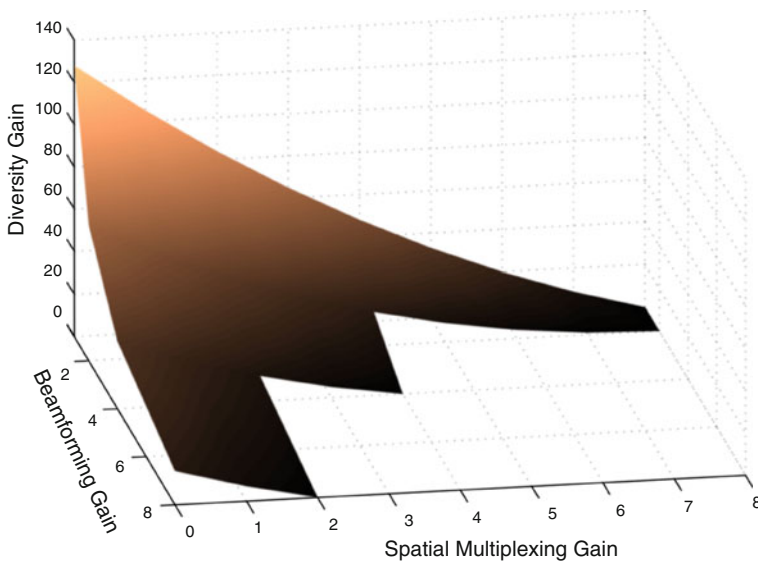


Fig. 3 Diversity-multiplexing-beamforming tradeoff of a 16×8 LSSTC with $m_k = 2$

find systems that has a trade-off curve to the left of the optimum trade-off curve, but not to his right.

Figure 3 shows the diversity-multiplexing-beamforming tradeoff of a 16×8 LSSTC system plotted in 3-D format. In the figure, it can be noted that increasing one parameter causes the other parameters to decrease and vice versa.

6 Numerical Results

In this section, the performance of the proposed single-user $N_T \times N_R$ LSSTC system is evaluated through numerous simulations and numerical results are presented. The channel model is a MIMO quasi-static Rayleigh flat-fading channel. The fading coefficients were

Table 2 Simulation parameters

Parameter	Value(s)
Transmitter mode	VBLAST, LSSTC
Total number of Tx antennas, N_T	4, 8, 16
Number of Rx antennas, N_R	2, 4, 8
Number of VBLAST layers, K	1, 2, 4, 8
Number of AAs per layer or STBC size, (m_k) , $k \in [1, \dots, K]$	2, 3, 4, 5, 6
Number of beam-steering elements in each AA, L	1, 2, 4, 8
Fading channel	quasi-static Rayleigh flat-fading
Data modulation	BPSK, QPSK, 16-QAM

generated using i.i.d. circular-complex normal random variables with zero-mean and 0.5 variance per dimension. The system model also assumes perfect CSI and DOA knowledge at the receiver and transmitter respectively. The most relevant parameters adopted in the simulations and the range of values they take are given in Table 2.

In all the Monte-Carlo simulations conducted in this work except Fig. 8, we used Alamouti's 2×2 STBC matrix of unity rate for the STBC encoders of each layer. At the transmitter, the total transmission power is normalized to one over the spatial and temporal domains; this power is distributed equally between the layers. In addition, unless otherwise mentioned, the SGIC detector does not perform ordering, rather it performs detection starting from the first layer in the \mathbf{H} matrix, which is not necessarily the best decoding order.

Figure 4a shows the effect of increasing the downlink beamforming gain by increasing the number of beam-steering elements L in each AA, while maintaining the same number of layers ($K = 2$) and AAs ($m_k = 2$), also the number of receive antennas is the same ($N_R = 2$). As shown in the figure, when the number of beam-steering elements L increases, the achievable SER performance significantly improves.

Figure 4b shows a fair comparison between LSSTC and VBLAST. This fairness is achieved by structure and spectral efficiency fairness, which means that the total number of antennas at the transmitter N_T and the number of symbols sent every time slot are the same for both systems. Figure 4b shows a comparison between LSSTC and VBLAST in terms of the symbol error rate. The two systems use a total number of transmit antennas, $N_T = 8$, and the receiver is equipped with 4 antennas. In this comparison we have also compared many transmitter configurations, in each a different modulation scheme is used such that the spectral efficiency would be the same for all of them, which is set to 4 bps/Hz. From Fig. 4b it can be clearly seen that VBLAST outperforms LSSTC in the low range of SNR, whereas for values of SNR that exceed 9 dB, the LSSTC outperforms VBLAST because it has a higher diversity order resulting from using STBC, which drives the SER to decay sharply.

Next, we propose an adaptive transmission scheme that selects the configuration and the modulation scheme in order to improve the performance. Table 3 lists the proposed transmitter configuration and modulation scheme depending on the SNR level.

For example if the SNR in a wireless system ranges from (6.6–9.2 dB), then the performance will be better if VBLAST scheme with 16-QAM modulation is used, while if it lies in the range(>9.2 dB) then it is better to use LSSTC scheme with 16-QAM modulation.

The adaptive scheme can be designed using an antenna array with the capability of electronically activating specific antenna elements and deactivating the remaining ones. This

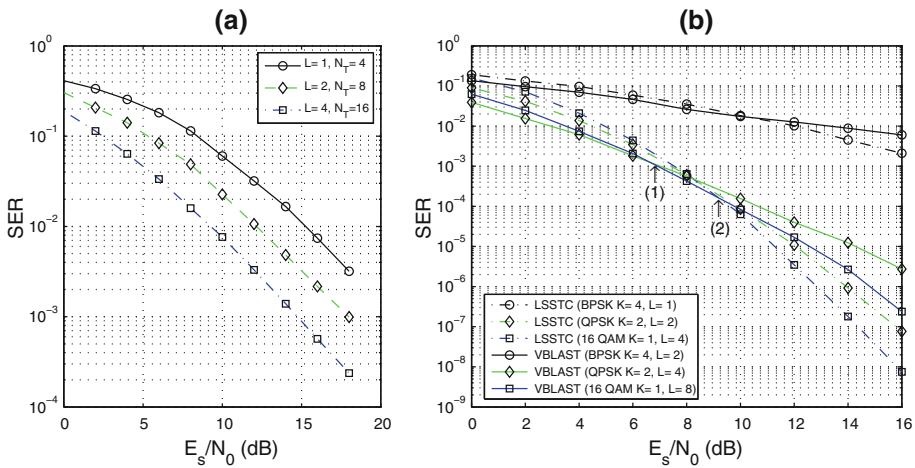


Fig. 4 **a** SER of LSSTC employing non-ordered SGIC and using 16-QAM modulation with $K = 2$ & $N_R = 2$ (comparing different number of beam-steering elements), and **b** SER of LSSTC employing non-ordered SGIC at 4 bps/Hz and different modulation schemes with $N_T = 8$ & $N_R = 4$ (comparing VBLAST to LSSTC fairly)

Table 3 Proposed transmitter configuration and modulation schemes

SNR level (dB)	Transmitter configuration	Modulation scheme
<6.6	VBLAST	QPSK
6.6–9.2	VBLAST	16-QAM
>9.2	LSSTC	16-QAM

is done to meet the antenna separation conditions of each mode in the multi-configuration system. In LSSTC, there are two conditions for the antenna element separation. (1) The AAs should be sufficiently far apart (greater than $\lambda/2$) in order to experience independent fading. (2) Beamforming elements within each AA should be spaced at small distance (less than $\lambda/2$) to achieve beamforming. On the other hand, VBLAST requires all the antennas to be spaced sufficiently far from each other.

Figure 5a compares the simulation results to the analysis results for the symbol error rate of an LSSTC system employing non-ordered SGIC and BPSK modulation with $K = 2$ and $N_R = 2$. It can be seen that the simulation and analysis results match quite well, which proves the validity of the analysis. Figure 5a proves the validity of approximating the equivalent noise $\mathbf{N}^{i,k}$ to a white Gaussian random variable

Figure 5b shows the SER of the individual layers of a 16×2 LSSTC employing a non-ordered SGIC detector with BPSK ($K = 2$ and $L = 4$) obtained from both simulation and analysis. The figure compares the analytical results obtained for LSSTC to those obtained from simulation. It is clear that the Monte Carlo simulation makes a nearly perfect match to the analysis results, which demonstrates the validity of the analysis proposed in this paper.

Figure 6 fairly compares LSSTC to VBLAST in terms of the outage capacity of an 8×4 MIMO using non-ordered SGIC at 15 dB average SNR. Several configuration are considered, and the capacity is plotted versus E_s/N_0 . As it can be seen from the figure, the capacity is approximately linearly increasing with increasing E_s/N_0 . It is clear to see that VBLAST outperforms LSSTC, which is actually expected, since VBLAST is a pure spatial multiplexing unlike LSSTC, where some antennas are assigned for diversity. An adaptive system can be

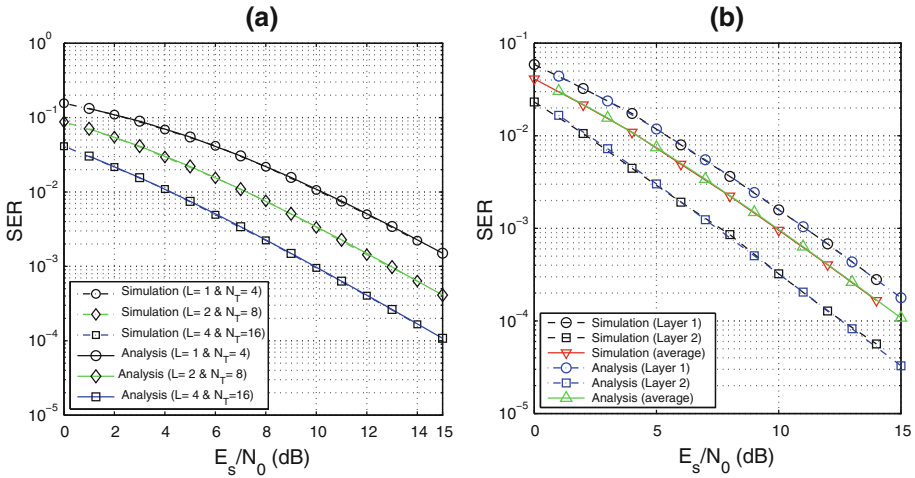


Fig. 5 **a** SER of LSSTC employing non-ordered SGIC and BPSK modulation with $K = 2$ & $N_R = 2$ (comparing analysis to simulation results), and **b** SER of the individual layers of a 16×2 LSSTC employing non-ordered SGIC and BPSK modulation with $K = 2$ & $L = 4$ (comparing analysis to simulation results)

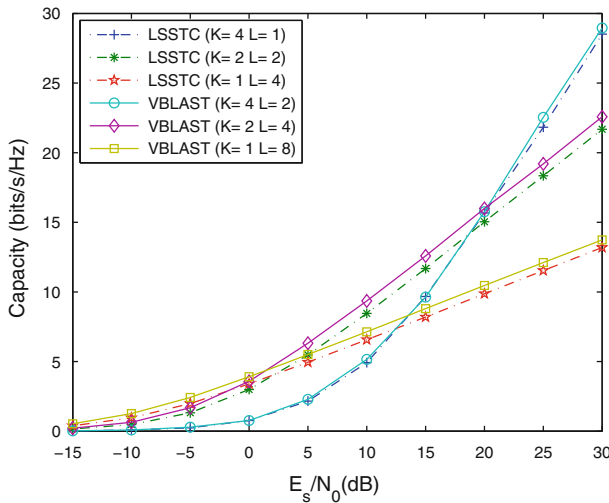


Fig. 6 Outage capacity versus SNR for an 8×4 MIMO at 10% outage probability, and 15 dB average SNR (comparing VBLAST to LSSTC fairly)

designed to maximize the capacity for all values of SNR. For the forementioned configuration we choose the single-layer VBLAST system for the first range (-15 dB up to 1 dB), and for the second range (1 dB up to 20 dB) the dual-layer VBLAST system gives the highest capacity. If the SNR lies in the last range (>20 dB), then using either LSSTC or VBLAST with 4 layers will have approximately the same capacity. However, Fig. 4b shows that LSSTC has a lower SER in the last range, and therefore, choosing LSSTC is better.

As discussed earlier, the first detected layer dominates the probability of error, therefore, we can approximate the average probability of error of the whole system by that of the first layer. In the following, we seek to further study the last statement, by comparing the SER of

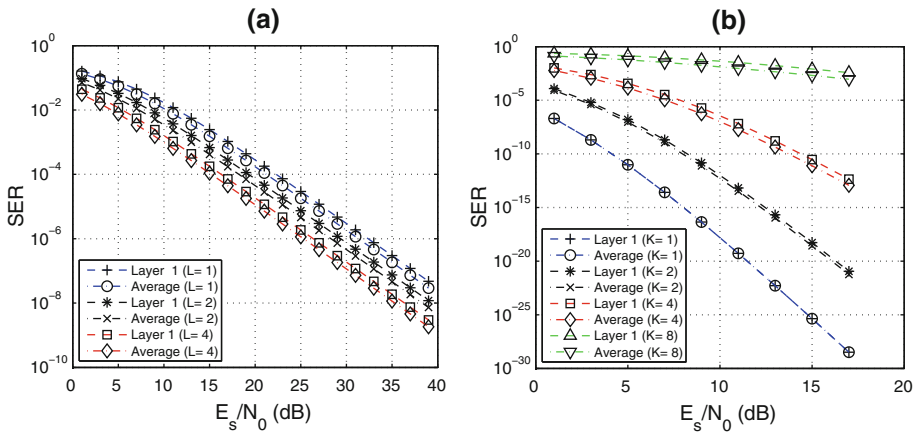


Fig. 7 **a** First layer & average SER of LSSTC employing SGIC and BPSK modulation with $K = 2$ & $N_R = 2$ & $m_k = 2$ (varying the number of beamforming elements (L)), and **b** first layer & average SER of LSSTC employing SGIC and BPSK modulation with $L = 2$ & $m_k = 2$ & $N_R = 8$ (varying the number of layers (K))

the first layer to the average SER, aiming to find which parameters or conditions will make this approximation much accurate.

Figure 7a shows the SER of LSSTC with varying the number of beamforming elements (L), where we can see that the gap between the first layer and the average doesn't change, and therefore it does not depend on L . Figure 7b shows the SER of LSSTC with varying the number of layers (K), and we can see that the gap between the first layer and the average increases with increasing K . In Fig. 8 the SER of LSSTC is plotted with varying the STBC size (m_k), $k \in [1, \dots, K]$, which corresponds to the number of AAs per layer. We can see that the gap between the first layer and the average decreases with increasing m_k . We can also note that the gap becomes constant when m_k becomes high, this is because the diversity order becomes high and the improvement does not change much after further increase in m_k .

7 Conclusions

In this paper, the performance of a single-user LSSTC was investigated. In particular, we extended the analysis of the probability of error for VBLAST systems employing QAM to include the effects of beamforming and STBC in a general LSSTC system. We showed that using antenna arrays in the LSSTC layers to provide beamforming results in a direct SNR gain, whereas STBCs in the LSSTC layers increases the diversity order of each layer. The analytical results were verified by the simulation results. Also, the instantaneous capacity of a single-user LSSTC was derived. Additionally, the tradeoff between diversity, multiplexing, and beamforming for LSSTC was investigated, which provides a deeper insight to the LSSTC system. The tradeoff analysis showed that increasing one parameter (e.g., diversity, multiplexing or beamforming) causes the other parameters to decrease according to the derived tradeoff. Finally, we proposed a multiconfiguration transmission scheme based on LSSTC and VBLAST systems. This scheme showed that LSSTC has a better performance than VBLAST at high SNR range.

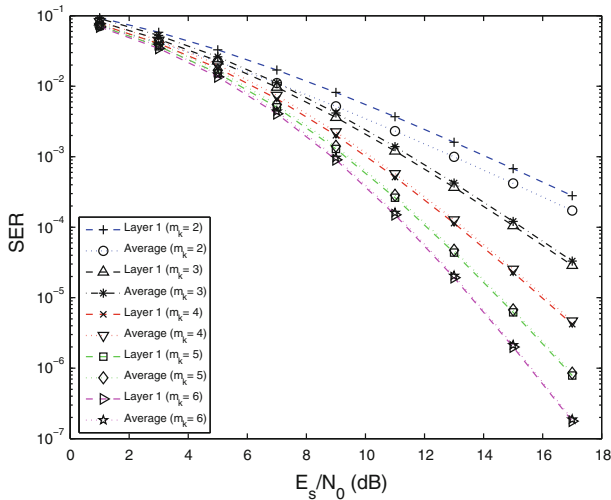


Fig. 8 First layer & average SER of LSSTC employing SGIC and BPSK modulation with $L = 2$ & $K = 2$ & $N_R = 2$ (varying the STBC size (m_k))

Acknowledgments The authors would like to acknowledge the support provided by King Fahd University of Petroleum and Minerals (KFUPM) under grant no. SB070005 and King Abdulaziz City for Science and Technology (KACST) through the Science and Technology Unit at KFUPM for funding this work through project number 08-ELE39-4 as part of the National Science, Technology and Innovation Plan.

References

1. Wolniansky, P. W., Foschini, G. J., Golden, G. D., & Valenzuela, R. A. (1998, October). V-BLAST: An architecture for realizing very high data rates over the rich-scattering wireless channel. In *URSI international symposium on signals, systems and electronics*, pp. 295–300.
2. Alamouti, S. (1998). A simple transmit diversity technique for wireless communications. *IEEE Journal on Selected Areas in Communications*, 16(8), 1451–1458.
3. Tarokh, V., Naguib, A., Seshadri, N., & Calderbank, A. (1999). Combined array processing and space-time coding. *IEEE Transactions on Information Theory*, 45(4), 1121–1128.
4. Mohammad, M., Al-Ghadhban, S., Woerner, B., Tranter, W. (2004) Comparing decoding algorithms for multi-layered space-time block codes. In *IEEE SoutheastCon proceedings*, pp. 147–152.
5. Chong, J. H., Khatun, S., Noordin, N. K., Ali, B. M., Syed, M. J. (2008) Joint optimal detection of ordering SIC ZF and SIC ZF MAP for V-BLAST/STBC wireless communication systems. In *ENICS '08: Proceedings of the international conference on advances in electronics and micro-electronics*, pp. 84–89.
6. El-Hajjar, M., Hanzo, L. (2007) Layered steered space-time codes and their capacity. *IEE Electronics Letters*, 43, 680–682.
7. Shen, C., Zhu, Y., Zhou, S., & Jiang, J. (2004) On the performance of V-BLAST with zero-forcing successive interference cancellation receiver. *IEEE Global Telecommunications Conference*, 2818–2822.
8. Loyka, S., & Gagnon, F. (2004). On BER analysis of the BLAST without optimal ordering over Rayleigh fading channel. *IEEE Vehicular Technology Conference*, 2, 1473–1477.
9. Shu, F., Lihua, L., Xiaofeng, T., & Ping, Z. (2007) A spatial multiplexing MIMO scheme with beamforming for downlink transmission. *IEEE Vehicular Technology Conference*, 700–704.
10. Tao, M., & Cheng, R. (2001). Low complexity post-ordered iterative decoding for generalized layered space-time coding systems. *IEEE International Conference on Communications*, 4, 1137–1141.
11. Salim, A. (2010). *Performance of layered steered space-time codes in wireless systems*. Master's thesis.
12. Al-Ghadhban, S. (2005). *Multi-layered space frequency Time Codes*. Ph.D. dissertation. Virginia, USA: Virginia Polytechnic Institute and State University.
13. Proakis, J. (2000). *Digital communications* (4th ed.). New York, USA: McGraw-Hill.

14. Al-Shalan, F. (2000). *Performance of quadrature amplitude modulation in Nakagami fading channels with diversity*, Ph.D. dissertation. Dhahran, Saudi Arabia: King Fahd University of Petroleum and Minerals.
15. Sandhu, S., & Paulraj, A. (2000). Space-time block codes: A capacity perspective. *IEEE Communications Letters*, 4(12), 384–386.
16. Al-Ghadhban, S., Buehrer, R., & Woerner, B. (2005) Outage capacity comparison of multi-layered STBC and V-BLAST systems. In *IEEE 62nd vehicular technology conference*, pp. 1:24–27.
17. Zheng, L., & Tse, D. N. C. (2003). Diversity and multiplexing: A fundamental tradeoff in multiple-antenna channels. *IEEE Transactions on Information Theory*, 49(5), 1073–1096.

Author Biographies



Ahmad S. Salim received his B.Sc. degree in Electrical Engineering from the University of Jordan, Amman, Jordan, in 2006. Later, he received his M.Sc. in Telecommunication Engineering from King Fahd University of Petroleum Minerals (KFUPM). He has achieved the eighth place in the University Qualifying Examination held in Jordan in the year 2005/2006 in the field of Electrical Engineering covering all the Jordanian universities. Currently, he's pursuing his Ph.D. in Electrical Engineering at Arizona State University, Arizona, United States. During this period, he had taught many courses and labs and has been actively participating in many committees in the department. His research interests include MIMO systems, space–time processing (LSSTC, STBC, VBLAST, etc.), cooperative communications, cognitive radio, multiuser diversity via scheduling, and OFDM-based IP networks such as LTE and WiMAX.



Salam A. Zummo received the B.Sc. and M.Sc. degrees in Electrical Engineering from King Fahd University of Petroleum & Minerals (KFUPM), Dhahran, Saudi Arabia, in 1998 and 1999, respectively. He received his Ph.D. degree from the University of Michigan at Ann Arbor, USA, in June 2003. He is currently an Associate Professor in the Electrical Engineering Department and the Dean of Graduate Studies at KFUPM. Dr. Zummo is a Senior Member of the IEEE. Dr. Zummo was awarded Saudi Ambassador Award for early Ph.D. completion in 2003, and the British Council/BAE Research Fellowship Awards in 2004 and 2006. He has more than 60 publications in international journals and conference proceedings in the area of wireless communications including error control coding, diversity techniques, MIMO systems, iterative receivers, multiuser diversity, multihop networks, user cooperation, interference modeling and networking issues for wireless communication systems.



Samir N. Al-Ghadhban received his Ph.D. in Electrical Engineering from Virginia Tech in 2005. He got his M.Sc. in Electrical Engineering from King Fahd University of Petroleum and Minerals (KFUPM) in Dhahran, Saudi Arabia in 2000. He also got his B.Sc. in Electrical Engineering (Highest Honors) in May 1997 from KFUPM, Dhahran, Saudi Arabia. His research interests are in wireless communications, MIMO systems, Compressive sensing and spectrum sensing.